ISSN 1674-1056
http://cpb.iphy.ac.cn
http://iopscience.iop.org/cpb
中国物理 B
Chinese Physics
中国物理 Chinese Physics B

Fabrication and characterization of one-port surface acoustic wave resonators on semi-insulating GaN substrates

Xue Ji(吉雪), Wen-Xiu Dong(董文秀), Yu-Min Zhang(张育民), Jian-Feng Wang(王建峰), Ke Xu(徐科)

Citation: Chin. Phys. B . 2019, 28(6): 067701. **doi:** 10.1088/1674-1056/28/6/067701
Journal homepage: http://cpb.iphy.ac.cn; http://iopscience.iop.org/cpb

What follows is a list of articles you may be interested in

Method of evaluating interface traps in Al_2O_3/AlGaN/GaN high electron mobility transistors

Si-Qin-Gao-Wa Bao(包斯琴高娃), Xiao-Hua Ma(马晓华), Wei-Wei Chen(陈伟伟), Ling Yang(杨凌), Bin Hou(侯斌), Qing Zhu(朱青), Jie-Jie Zhu(祝杰杰), Yue Hao(郝跃)

Chin. Phys. B . 2019, 28(6): 067304. **doi:** 10.1088/1674-1056/28/6/067304

Aging mechanism of GaN-based yellow LEDs with V-pits

Tian-Ran Zhang(张天然), Fang Fang(方芳), Xiao-Lan Wang(王小兰), Jian-Li Zhang(张建立), Xiao-Ming Wu(吴小明), Shuan Pan(潘栓), Jun-Lin Liu(刘军林), Feng-Yi Jiang(江风益)

Chin. Phys. B . 2019, 28(6): 067305. **doi:** 10.1088/1674-1056/28/6/067305

Mechanism of Ti/Al/Ni/Au ohmic contacts to AlGaN/GaN heterostructures via laser annealing

Mingchen Hou(侯明辰), Gang Xie(谢刚), Kuang Sheng(盛况)

Chin. Phys. B . 2019, 28(3): 037302. **doi:** 10.1088/1674-1056/28/3/037302

Propagations of Rayleigh and Love waves in ZnO films/glass substrates analyzed by three-dimensional finite element method

Yan Wang(王艳), Ying-Cai Xie(谢英才), Shu-Yi Zhang(张淑仪), Xiao-Dong Lan(兰晓东)

Chin. Phys. B . 2017, 26(8): 087703. **doi:** 10.1088/1674-1056/26/8/087703

Transparent ZnO/glass surface acoustic wave based high performance ultraviolet light sensors

Wang Wen-Bo, Gu Hang, He Xing-Li, Xuan Wei-Peng, Chen Jin-Kai, Wang Xiao-Zhi, Luo Ji-Kui

Chin. Phys. B . 2015, 24(5): 057701. **doi:** 10.1088/1674-1056/24/5/057701

Fabrication and characterization of one-port surface acoustic wave resonators on semi-insulating GaN substrates*

Xue Ji(吉雪)[1,2], Wen-Xiu Dong(董文秀)[2], Yu-Min Zhang(张育民)[1,2], Jian-Feng Wang(王建峰)[2], and Ke Xu(徐科)[2,3,†]

[1] School of Nano Technology and Nano Bionics, University of Science and Technology of China, Hefei 230026, China
[2] Suzhou Institute of Nano-Tech and Nano-Bionics, Chinese Academy of Sciences, Suzhou 215123, China
[3] School of Information Science and Technology, University of Science and Technology of China, Hefei 230026, China

(Received 10 December 2018; revised manuscript received 7 March 2019; published online 8 May 2019)

One-port surface acoustic wave resonators (SAWRs) are fabricated on semi-insulating high-quality bulk GaN and GaN film substrates, respectively. The semi-insulating GaN substrates are grown by hydride vapor phase epitaxy (HVPE) and doped with Fe. The anisotropy of Rayleigh propagation and the electromechanical coupling coefficient in Fe-doped GaN are investigated. The difference in resonance frequency between the SAWs between [11$\bar{2}$0] GaN and [1$\bar{1}$00] GaN is about 0.25% for the Rayleigh propagation mode, which is smaller than that of non-intentionally doped GaN film (~1%) reported in the literature. The electromechanical coupling coefficient of Fe-doped GaN is about 3.03%, which is higher than that of non-intentionally doped GaN film. The one-port SAWR fabricated on an 8-μm Fe-doped GaN/sapphire substrate has a quality factor of 2050, and that fabricated on Fe-doped bulk GaN has a quality factor as high as 3650. All of our results indicate that high-quality bulk GaN is a very promising material for application in SAW devices.

Keywords: surface acoustic wave, one-port resonator, gallium nitride (GaN), semi-insulating, Fe-doped

PACS: 77.65.Dq, 73.61.Ey, 81.05.Ea **DOI:** 10.1088/1674-1056/28/6/067701

1. Introduction

Surface acoustic wave (SAW) devices such as filters, resonators, and oscillators have been used in various areas, including wireless communication, radio frequency identification (RFID) and sensing applications.[1–3] Substrate materials are of great importance for the performance of SAW devices. Piezoelectric substrates, such as $LiNbO_3$, $LiTaO_3$, and quartz crystals, are widely used to fabricate the SAW resonators and filters. To enhance the performance of SAW devices, III-nitride semiconductors, such as GaN and AlN, with excellent optical, electrical and acoustical properties, are also expected to be used to prepare the monolithic SAW devices.[4]

The GaN substrate has received great attention due to its good piezoelectric properties, high mechanical and chemical stability. The phase velocity of SAW on GaN is close to 3800 m/s, which is higher than those on quartz (∼ 3150 m/s), GaAs (∼ 2470 m/s) and $LiNbO_3$ (∼ 3480 m/s).[5] Consequently, it is a perfect alternative to the fabrication of high-frequency SAW devices of up to 2 GHz by conventional photolithography. Moreover, the SAW devices on GaN can work in a harsh environment (e.g., high temperature and high voltage) for a long time, which makes it is possible for them to be widely used in a power monitoring system.[6,7]

In the traditional heteroepitaxial growth of GaN on foreign substrates, the GaN film thickness and quality are very limited, while the development of GaN based SAW devices is greatly hindered by the availability of high-quality material with high resistivity. However, SAW delay lines have been fabricated and characterized on semi-insulating bulk GaN substrate. Zhou *et al.* reported a GaN SAW delay line resonator at about 2 GHz, which was fabricated on a semi-insulating self-standing GaN substrate.[8] The insertion loss of GaN SAW delay line is −10 dB in this report, which is higher than that of SAW delay line on GaN film (lower than −30 dB). However, there are fewer reports about the one-port SAW resonators based on semi-insulating bulk GaN. One-port SAW resonators, which are the foundation for designing and optimizing SAW devices, have been extensively studied and used in various fields. The main parameters for resonators are resonant frequency and quality factor (Q). High-frequency SAW resonators can be used in fixed frequency oscillators, narrow band modulation oscillators and wireless sensors, while high-quality factor SAW resonators can be used in low phase noise designs.[9]

Recently, our group has realized bulk GaN growth by the hydride vapor phase epitaxy (HVPE), and high-resistivity bulk GaN can be achieved by Fe doping.[10] This makes it possible for us to explore the characteristics of SAW fabricated on bulk semi-insulating GaN. In this article, one-port SAW resonators are fabricated and characterized on semi-

*Project supported by the National Key Research and Development Program of China (Grant No. 2017YFB0403002), the National Science Fund for Distinguished Young Scholars, China (Grant No. Y3CHC11001), and the National Natural Science Foundation of China (Grant No. 11604368).

†Corresponding author. E-mail: kxu2006@sinano.ac.cn

© 2019 Chinese Physical Society and IOP Publishing Ltd

insulating GaN grown by HVPE and doped with Fe. The relevant device properties are then investigated. It is found that the anisotropy of Rayleigh propagation is smaller than that of non-intentionally doped GaN film and the electromechanical coupling coefficient in Fe-doped GaN is higher than that of non-intentionally doped GaN film. Moreover, a one-port SAWR fabricated on an Fe-doped bulk GaN substrate exhibits a higher quality factor than that on an 8-μm Fe-doped GaN/sapphire substrate. In addition, the temperature coefficient of frequency (TCF) of Fe-doped bulk GaN substrate is slightly lower than that of GaN film. This implies that high-quality bulk GaN is a very promising material for applications in SAW devices, especially high-temperature sensing.

2. Experimental details

To fabricate SAW devices, high-resistivity bulk GaN is needed. The resistivity of GaN substrate is an important factor for surface acoustic modes and electromechanical coupling coefficients (k^2_{eff}).[11–14] Fe-dopant is typically used as stable deep acceptor impurities to obtain high-resistivity GaN substrates.[10,14,15] In this study, Fe-doped semi-insulated bulk GaNs and GaN films were grown by the home-made HVPE technique that was provided by Suzhou Nanowin Science and Technology Company, China. The thickness of bulk GaN was above 350 μm. The GaN films were grown on (0001) sapphire substrate with a thickness of 8 μm. The resistivities of the two GaN substrates were both higher than 10^8 Ω·cm. The crystal quality of the GaN substrates was investigated by high resolution x-ray diffraction (Bruker, D8 Discover). The dislocation density values of the two GaN substrates were both lower than 2×10^7 cm^{-2}. Meanwhile, a homogeneous surface of substrate material was also critical for low propagation loss and it was evaluated by the root mean square (RMS) roughness.[16] The surface morphology of bulk GaN and GaN film were measured by atomic force microscopy (AFM, Dimension ICON). As indicated in Fig. 1, a homogeneous surface with an RMS roughness of about 1 nm was obtained.

The one-port SAW resonator consisted of one interdigital transducer (IDT) and two identical symmetrical reflectors. The IDT was located inside the reflectors as shown in Fig. 2(a). The IDT had 50 pairs of electrodes with a width and gap of 2 μm, *i.e.*, the periodicity of 8 μm. The reflectors contained 500 short-circuited gratings and the distance (L_g) between IDT and reflector was in a range of (5-1/8) λ. The acoustic aperture (W) was 100λ. The structures were prepared by means of electron-beam evaporation. The metal structure is 30-nm nickel (Ni), which was used as an adhesion layer, and 80-nm gold (Au), which formed a Schottky contact and was lithographically structured by standard lift-off technique. The detailed SEM image of the IDT fingers is shown in Fig. 2(b). The S parameters (the logarithm of the ratio of output energy to input energy) of the resonators were measured by a vector network analyzer (Agilent E5071C) with a micro-probe station at room temperature and atmosphere.

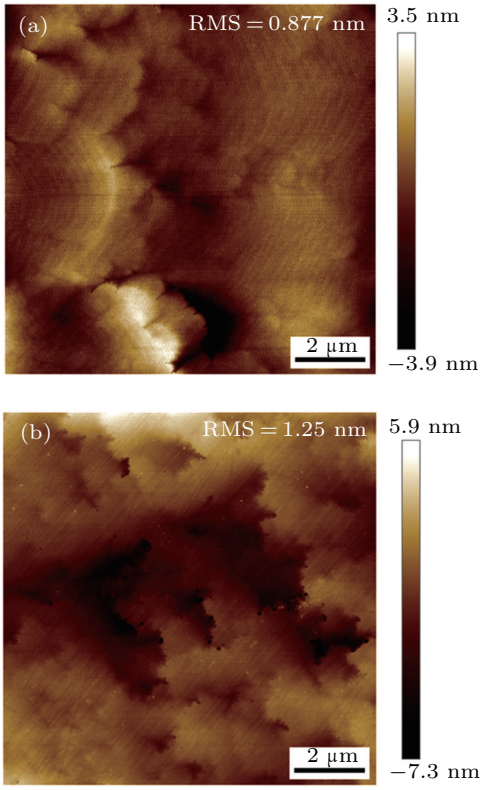


Fig. 1. (a) Surface property of bulk GaN by AFM in a range of 10 μm×10 μm, (b) AFM image of GaN film in a range of 10 μm×10 μm.

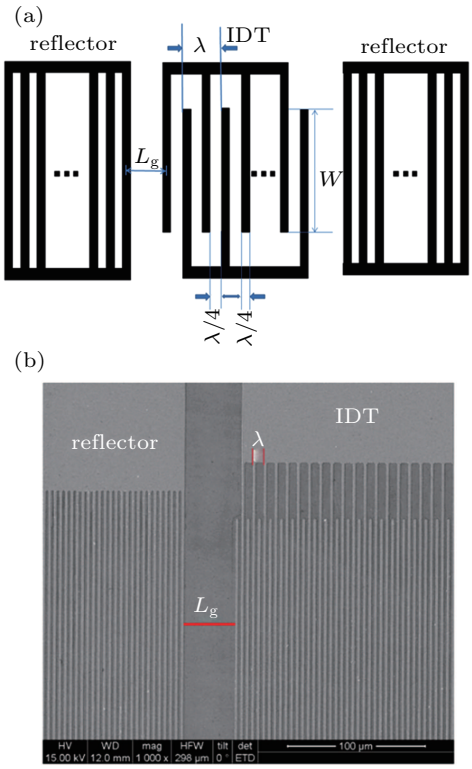


Fig. 2. (a) Schematic presentation of one-port SAWR, and (b) SEM image of IDT fingers.

3. Results and discussion

To analyze the influence of the SAW propagation direction on the bulk GaN, two one-port SAWRs are processed in two vertical directions of bulk GaN substrate. In one resonator, the SAWs propagate in the [11$\bar{2}$0] direction corresponding to direction A; while in another resonator, the SAW propagates along the [1$\bar{1}$00] direction corresponding to direction B as indicated in Fig. 3(a). The performance of the resonator is characterized by its admittance. In Fig. 3(b), the SAWs propagate in direction A, the fundamental resonance mode—which corresponds to the maximum value of the admittance at 474.81 MHz—and the anti-resonance mode—which corresponds to the minimum value of the admittance at 475.26 MHz. Figure 3(c) shows that the fundamental resonance mode and the anti-resonance mode at 473.68 MHz and 473.97 MHz, respectively, corresponding to SAWs propagating in direction B. The response center frequencies of these two resonators are very close. The SAW velocity (V_{SAW}) can be calculated according to the following equation:

$$V_{\mathrm{SAW}} = f \cdot \lambda. \tag{1}$$

From the resonance frequency and the wavelength, we obtain $V_{\mathrm{SAW}} \approx 3800$ m/s. So the frequencies that we have detected correspond to the fundamental Rayleigh (R) mode in GaN.

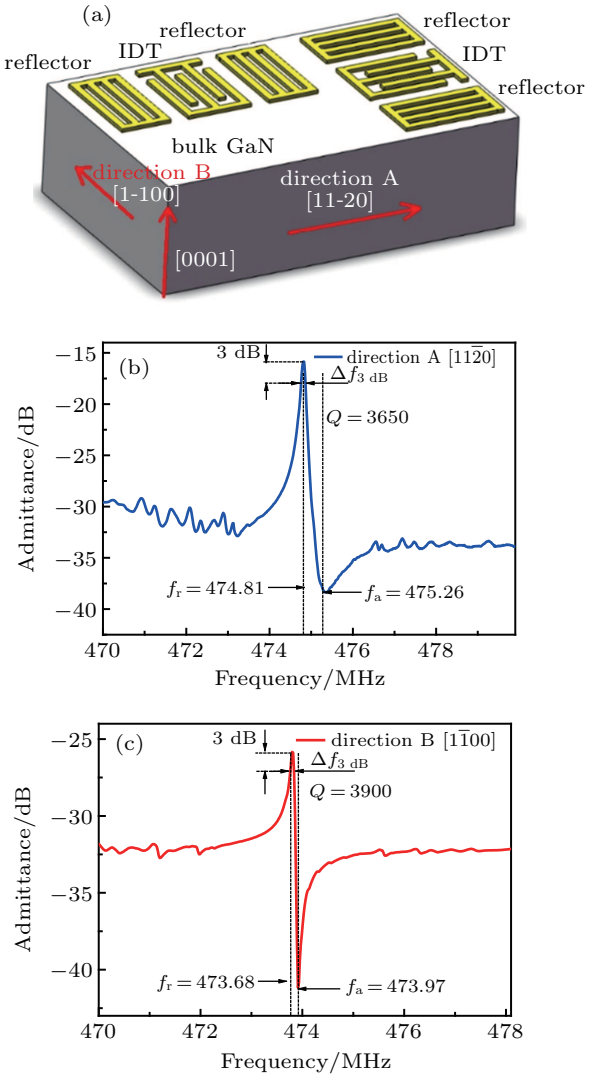


Fig. 3. (a) Orientations of SAWRs on GaN wafer. For resonators in direction A, acoustic waves propagate along [11$\bar{2}$0] direction. While in direction B, acoustic waves propagate along [1$\bar{1}$00] direction. (b) Admittance of SAWs propagating along [11$\bar{2}$0] direction. (c) Admittance of SAWs propagating along [1$\bar{1}$00] direction.

Compared with the [1$\bar{1}$00] direction, a higher value of the resonance frequency is observed for the [11$\bar{2}$0] direction of the acoustic wave. The difference in resonance frequency between the SAWs from [11$\bar{2}$0] and [1$\bar{1}$00] is about 0.25% for the Rayleigh propagation mode. Muller *et al.*[7] and Calle *et al.*[17] have obtained even bigger results (about 1%) for a GaN membrane grown on sapphire regarding the Rayleigh propagation mode. The substrate material may also induce SAWs to anisotropically propagate. The GaN has a wurtzite crystal structure, point group 6 mm, which leads to isotropically elastic and piezoelectric properties in the *c* plane. However, the trigonal crystal class of sapphire −3 m is non-piezoelectric and shows a 6-fold symmetry of the elastic properties in the *c* plane. This crystal mismatch induces a dependence of the SAW frequency on orientation.[17] High-crystal quality bulk GaN is a bulk substrate material. Compared with epitaxial films, its crystal mismatch is smaller than that of thin film substrate material. Consequently, the difference in SAW velocity between two different directions is also smaller than that of thin film material. Therefore, the difference in frequency between the two directions is smaller.

The electromechanical coupling coefficient (K^2_{eff}) is also assessed in this work, which is a measure of energy conversion efficiency between the electrical domain and the mechanical domain. A high K^2_{eff} value means a high energy conversion efficiency. To explore the piezoelectric properties of GaN substrate, the K^2_{eff} of the device is calculated from[18]

$$K^2_{\mathrm{eff}} = \frac{2(v_0 - v_{\mathrm{m}})}{v_0} = \frac{\pi}{4N}\frac{G(f_{\mathrm{r}})}{B(f_{\mathrm{r}})}, \tag{2}$$

where v_0 and v_{m} are the SAW phase velocity along the free surface and the SAW phase velocity along the electrically short-circuited surface of the GaN substrate, respectively. The electromechanical coupling coefficient is calculated by the radiation conductance $G(f_{\mathrm{r}})$ and the susceptance $B(f_{\mathrm{r}})$, which are derived from Smith's equivalent model by measuring S_{11} parameter (reflection) at response center frequency; N is the number of finger pairs of the IDT. At room temperature, the mean value of K^2_{eff} that we obtained for the Fe-doped GaN substrate is about 3.03% in the [11$\bar{2}$0] direction and also in the [1$\bar{1}$00] direction. The K^2_{eff} that we measured is also larger than some other published results, which are generally considered between 0.1% and 1.9% with different thickness and different resistivities.[19–21] Lee *et al.* reported that the K^2_{eff} of Mg-doped GaN film grown on (0001) sapphire by MOCVD

is about 4.3%.[22] It is shown that the Fe-doped GaN substrate has a high $K^2_{\rm eff}$ value, suggesting a high energy-conversion efficiency, which is beneficial to the Q-factor. The Q-factor of the SAW resonator is evaluated by its SAW propagation loss. For the acoustic device, the Q-factor and SAW propagation loss α is related by[23,24]

$$\alpha\,(\mathrm{dB}/\lambda) = \frac{8.686\pi f_{\rm r}}{Q f_{\rm g}}, \tag{3}$$

where $f_{\rm r} = v_{\rm p}/\lambda_0$ and $f_{\rm g} = v_{\rm g}/\lambda_0$ with λ_0 being the wavelength of SAW, $v_{\rm p}$ the SAW phase velocity, and $v_{\rm g}$ SAW group velocity. When the electromechanical coupling coefficient is larger, it represents a higher piezoelectric effect and more energy is converted into acoustic energy of the SAW device, the propagation loss is reduced, and the Q-factor is increased, relatively.

The Q-factor of one-port SAWR is a measure of the energy loss in the period and significantly influences the insertion loss and rectangle coefficient in SAW device applications.[25] The most basic definition of Q-factor is

$$Q = 2\pi \frac{E_{\rm s}}{E_{\rm d}}, \tag{4}$$

where $E_{\rm s}$ is the energy stored in the system and $E_{\rm d}$ is the energy dissipated per radian of the vibration cycle. Several methods can be used to estimate the Q-factor practically. The Q-factor characterizes the sharpness of the resonance peak and is defined by the ratio of the resonance frequency to the 3-dB bandwidth and is expressed as

$$Q_{\rm r} = \frac{f_{\rm r}}{\Delta f_{3\ \mathrm{dB}}}. \tag{5}$$

The calculated $Q_{\rm r}$ values of the fundamental resonance mode are 3650 and 3900, corresponding to SAWs propagate along the [11$\bar{2}$0] and [1$\bar{1}$00], respectively. For the bulk GaN substrate, the one-port resonator fabricated on it has a high Q-factor and the Q values of the one-port SAWRs are above 3600 in the two different crystal orientations.

To ensure good comparison, we fabricate a one-port resonator with the same structure on Fe-doped GaN film in the [11$\bar{2}$0] direction, and the various parameters remain unchanged. As shown in Fig. 4(a), the resonant frequency of the SAWR on Fe-doped GaN film is detected at 471.20 MHz. The resonant frequency drops by about 3 MHz, which may be due to various accidental factors in the device fabrication process. The reflection coefficient (S_{11}) measured by VNA represents the ratio of reflected signal energy to incident signal energy, which is usually shown in unit dB. It does not characterize the size of energy loss directly. A small S_{11} value represents that the reflected signal energy is small. It also suggests that there is a large energy absorption in the SAW device. This means that more energy is stored in the resonators that we have fabricated. In Fig. 4(a), the S_{11} of resonator fabricated on the bulk GaN is smaller than that on the GaN film. This means that the more energy is stored in the resonators fabricated on the bulk GaN, while the signal in the resonator fabricated on the bulk GaN is better than that in the resonator fabricated on GaN film. These results indicate that the Q-factor on the bulk GaN is higher than that on GaN film. Furthermore, the Q value of device fabricated on the Fe-doped GaN film is significantly reduced, generally around 2000; as shown in Fig. 4(b). More energy absorption in the resonator is one of the reasons why the one-port SAWR on the bulk GaN has a higher Q-factor than that on the GaN film.

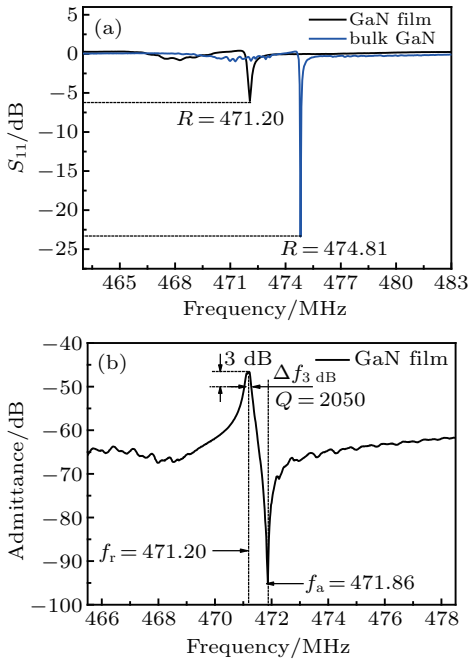


Fig. 4. (a) Frequency response of two SAW one-port resonators, both acoustic waves propagate along the [11$\bar{2}$0]. (b) Admittance of one-port SAW resonator on GaN film, and the acoustic waves propagates along the [11$\bar{2}$0].

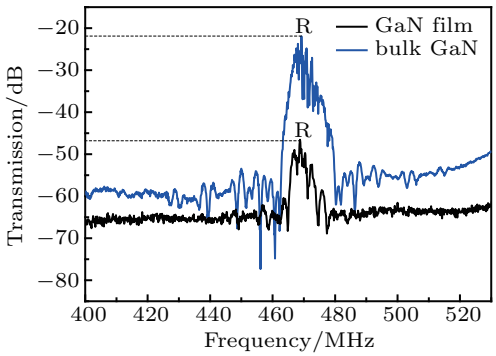


Fig. 5. Transmission characteristics of two SAW delay lines. SAW devices are based on GaN film and bulk GaN, respectively. Wavelengths for both delay lines are 8 μm. The resonance marked by R located at about 470 MHz is Rayleigh mode.

The Q-factor of one-port SAW resonator mostly depends on the energy loss of the SAW propagation process, which can be evaluated by S_{21} parameter. A high S_{21} value means a low energy loss. Then, a delay line SAW device of the same structure is fabricated on both substrates. As shown in Fig. 5, it is found that the insertion loss of the delay line on the bulk GaN is much higher than that of the GaN film. It is very likely that the device produced on the high-crystal quality bulk GaN

has a small SAW propagation loss, which leads to a significant increase in quality factor in Fig. 4. The propagation loss is related to the material and the resonator structure. The most important part is the propagation path loss of the SAW on the substrate material surface, including absorption loss, scattering loss and dispersion loss. It is very likely that the device produced on the high-crystal quality bulk GaN has a small propagation loss, which leads to a significant increase in quality.

Considering the thermal stability of the one-port SAWRs, the temperature coefficient of frequency (TCF) is calculated for the Rayleigh mode of the one-port SAW resonator from the following equation:

$$\mathrm{TCF} = \frac{1}{f_0}\frac{\mathrm{d}f}{\mathrm{d}T} = \frac{1}{T - 25\ ^\circ\mathrm{C}}\frac{f(T) - f(25\ ^\circ\mathrm{C})}{f(25\ ^\circ\mathrm{C})}, \tag{6}$$

where T is the temperature in Celsius and $f(T)$ denotes the resonance frequency at T. Two SAWRs based on different substrates are examined in a temperature range from 25 °C to 150 °C. Figure 6 shows the variations of response frequency with temperature of two one-port resonators. As the temperature increases, whether a GaN film substrate is used or a bulk GaN substrate is adopted, the resonant frequencies of the two SAWRs based on two substrates gradually decrease. It can be seen that both resonant frequencies linearly decrease, and the downward trend of the bulk GaN substrate is slightly larger than that of the GaN film. According to formula (5), we can calculate the TCFs of the two substrates, which are −22.8 ppm/°C and −23.8 ppm/°C, respectively. The TCF of bulk GaN substrate is slightly lower than that of GaN film, and large enough to be used in temperature sensors. All of our results suggest that SAWR fabricated on bulk GaN is sensitive to high temperature monitoring.

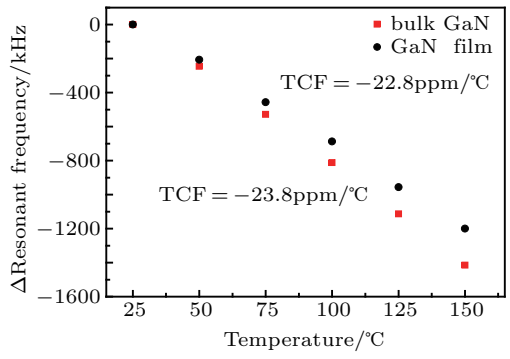


Fig. 6. The change in resonant frequency with temperature of SAWRs based on GaN film and bulk GaN.

4. Conclusions

In this work, the properties of one-port SAWRs fabricated on semi-insulating Fe-doped GaN substrates are investigated. The transmission characteristics of the Rayleigh mode are evaluated in two vertical propagation directions, *i.e.*, [11$\bar{2}$0] GaN and [1$\bar{1}$00] GaN. The electromechanical coupling coefficient for the Rayleigh mode is 3.03%, and the quality factor is above 3600 for the resonator fabricated on semi-insulating bulk GaN, which is a high value for the quality factor of GaN SAW device. The temperature coefficient of frequency for bulk GaN SAWR is slightly lower than that for the device fabricated on GaN film grown on sapphire substrate, indicating that it has potential in high-temperature sensing applications. It is shown that the high-quality bulk semi-insulating GaN will open up a new method to fabricate GaN SAW devices.

Acknowledgment

The authors would like to thank the Platform of Characterization and Test, Suzhou Institute of Nano-Tech and Nano-Bionics, Chinese Academy of Sciences.

References

[1] Wang W S, Tsai C J and Ma C C 2013 *J. Appl. Phys.* **114** 064911
[2] Fu C, Elmazria O, Sarry F, Mahalingam T, Yang S S and Lee K 2014 *Sens. Actuators A: Phys.* **220** 270
[3] Wang W B, Gu H, He X L, Xuan W P, Chen J K, Wang X Z and Luo J K 2015 *Chin. Phys. B* **24** 057701
[4] Miškinis R, Jokubauskis D, Urba E, Smirnov D, Gaidamovičiūtė L, Mikalauskas K, Sereika A, Rimeika R and Čiplys D 2015 *Acta Phys. Pol. A* **127** 90
[5] Rais-Zadeh M, Gokhale V J, Ansari A, Faucher M, Theron D, Cordier Y and Buchaillot L 2014 *J. Microelectromech. Syst.* **23** 1252
[6] Lu X, Ma J, Yue C P and Lau K M 2013 *IEEE Microwave Wireless Compon. Lett.* **23** 318
[7] Muller A, Konstantinidis G, Giangu I, Adam G C, Stefanescu A, Stavrinidis A, Stavrinidis G, Kostopoulos A, Boldeiu G and Dinescu A 2017 *IEEE Sens. J.* **17** 7383
[8] Zhou J, Li L, Lu H, Kong C, Kong Y, Chen T and Chen C 2014 *Proceedings of* 2014 *3rd Asia-Pacific Conference on Antennas and Propagation (Apcap* 2014*)* 1348
[9] Lakin M, Kline G R and McCarron K T 1993 *IEEE Trans. Microwave Theory Tech.* **41** 2139
[10] Xu K, Wang J F and Ren G Q 2015 *Chin. Phys. B* **24** 066105
[11] Soluch W and Brzozowski E 2014 *IEEE Trans. Electron. Dev.* **61** 3395
[12] Petroni S, Tripoli G, Combi C, Vigna B, De Vittorio M, Todaro M T, Epifani G, Cingolani R and Passaseo A 2004 *Superlattices Microstruct.* **36** 825
[13] O'Clock G D and Duffy M T 1973 *Appl. Phys. Lett.* **23** 55
[14] Fan Y, Liu Z, Xu G, Zhong H, Huang Z, Zhang Y, Wang J and Xu K 2014 *Appl. Phys. Lett.* **105** 062108
[15] Zhang M, Zhou T F, Zhang Y M, Li B, Zheng S N, Huang J, Sun Y P, Ren G Q, Wang J F, Xu K and Yang H 2012 *Appl. Phys. Lett.* **100** 041904
[16] Xiao X, Tao Y and Sun Y 2014 *Chin. Phys. B* **23** 106803
[17] Calle F, Pedrós J, Palacios T and Grajal J 2005 *Phys. Status Solidi (c)* **2** 976
[18] Yang S, Ai Y, Zhang Y, Cheng Z, Zhang L, Jia L, Dong B, Zhang B and Wang J 2018 *J. Micromech. Microeng.* **28** 085005
[19] Chen Z, Lu D C, Wang X H, Liu X L and Han P D 2001 *Chin. Phys. Lett.* **18** 1418
[20] Rimeika R, Ciplys D, Shur M S, Gaska R, Khan M A and Yang J 2002 *Phys. Status Solidi (b)* **234** 897
[21] Deger C, Born E, Angerer H, Ambacher O, Stutzmann M, Hornsteiner J, Riha E and Fischerauer G 1998 *Appl. Phys. Lett.* **72** 2400
[22] Lee S H, Jeong H H, Bae S B, Choi H C, Lee J H and Lee Y H 2001 *IEEE Trans. Electron. Dev.* **48** 524
[23] Fujii S, Odawara T, Yamada H, Omori T, Hashimoto K Y, Torii H, Umezawa H and Shikata S 2013 *IEEE Trans. Ultrason Ferroelectr. Freq. Control* **60** 986
[24] Shu L, Peng B, Li C, Gong D, Yang Z, Liu X and Zhang W 2016 *Sensors* (Basel) **16**
[25] Razavi B 1996 *IEEE J. Solid-State Circuits* **31** 331